JACS
JOURNAL OF THE AMERICAN CHEMICAL SOCIETY
Article
pubs.acs.org/JACS

Iodine (I_2) as a Janus-Faced Ligand in Organometallics

Andrey Yu. Rogachev and Roald Hoffmann*

Baker Laboratory, Department of Chemistry and Chemical Biology, Cornell University, Ithaca, New York 14853, United States

Supporting Information

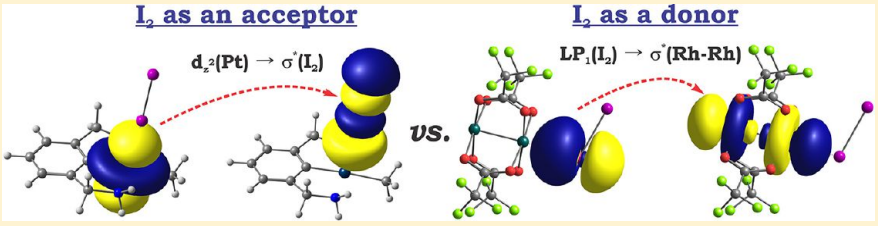

ABSTRACT: The four known diiodine complexes have distinct geometries. These turn out, as we demonstrate by a bonding analysis, to be a direct consequence of diiodine acting as an acceptor in one set, the van Koten complexes, and as a donor in the Cotton, Dikarev, and Petrukhina extended structure. The primary analytical tool utilized is perturbation theory within the natural bond orbital (NBO) framework, supported by an energy decomposition analysis. The study begins by delineating the difference between canonical molecular orbitals (MOs) and NBOs. When iodine acts as an acceptor, bonding collinearly in the axial position of a square-planar d^8 Pt(II) complex, the dominant contributor to the bonding is a σ^*(I−I) orbital as the acceptor orbital, while a mainly d_z^2 orbital centered on the metal center is the corresponding donor. That this kind of bonding is characteristic of axial bonding in d^8 complexes was supported by model calculations with incoming donors and acceptors, NH_3 and BH_3. In contrast, the distinct "bent" coordination of the I_2 bound at the axial position of the $[Rh_2(O_2CCF_3)_4]$ paddle-wheel complex is associated with a dominant donation from a p-type lone pair localized on one of two iodine atoms, the σ^*(Rh−Rh) antibonding orbital of the metal complex acting as an acceptor orbital. We check the donor capabilities of I_2 in some hypothetical complexes with Lewis acids, H^+, $AlCl_3$, $B(CF_3)_3$. Also, we look at the weakly bound donor−acceptor couple $[(I_2)\cdot(I_2)]$. We explore the reasons for the paucity of I_2 complexes and propose candidates for synthesis.

INTRODUCTION

Bristling with Lewis base functionality, their lone pairs, one would expect that dihalogens (X_2, X = F, Cl, Br, I) would be excellent ligands in transition metal complexes. Yet such compounds are most rare.[1] Also rare, but somewhat more abundant, are metal complexes in which a ligand acts as an acceptor, a Lewis acid, and not a donor. One might think these two kinds of oddity would have no intersection, but they do. We tell here the remarkable story of I_2, a ligand that bridges these two rare categories. In two of the few well-characterized transition metal complexes of dihalogens, **1** and **2** (Figure 1a,b), the bonding is, as we will show, completely different. In one of them, the van Koten compounds,[2] I_2 bonds predominantly as an acceptor, while in others, as a donor,[3] with well-delineated stereochemical consequences. An extensive literature search revealed only two further crystallographically characterized organometallic complexes of I_2 (Figure 1c,d),[4,5] one a very recent example. In both of them, iodine bonds as an acceptor, as in the van Koten compounds.[2]

The description of a ligand as a donor or an acceptor has always had attached to it a degree of ambiguity. Consider the protonation of a transition metal complex. There are two extreme perspectives of what happens on diprotonation of, for example, $Fe(CO)_4^{2-}$: one is that a Lewis acid, H^+, protonates the metal-based lone pair of a tetrahedral d^{10} complex; the other is that two electrons are transferred on bonding (time and space unspecified) to H^+, oxidizing the metal, making the ligand H^-, so that one has an octahedral d^6 Fe(II) complex. The truth is in between, of course, and the geometry of $Fe(CO)_4H_2$ is partway between a tetrahedral and octahedral one.[6]

Putting such clear ambiguities of oxidation and reduction aside, they would exist for super Lewis acids (BR_3) and Lewis bases (ER_3^-, E = group 14) alike, one is left with a handful of cases of ligands that bind in a primarily acceptor fashion to a transition metal. The work of the Eisenstein group on SnH_3 coordination[7] as well as recent studies of the Gabbaï group,[8] point to this kind of bonding, as does an older organometallic story, that of SO_2 complexes.[9] This small molecule can bond as a donor or an acceptor, with different geometrical consequences. The SO_2 complexes form a distinct parallel to the I_2 bonding we describe.

The van Koten compound is a relatively uncommon 5-coordinate Pt(II) complex. While the 16-electron nature of the Pt(II) complex in principle allows coordination of a fifth ligand, the linear end-on coordination of diatomic iodine, occupying the fifth axial position (Scheme 1A), does not "follow" in its directionality the frontier orbital lone pair(s) of I atoms, were one to assume I_2 is a donor here. The HOMO of I_2 is a π^*

Received: December 25, 2012
Published: February 5, 2013

   dx.doi.org/10.1021/ja312584u | J. Am. Chem. Soc. 2013, 135, 3262−3275

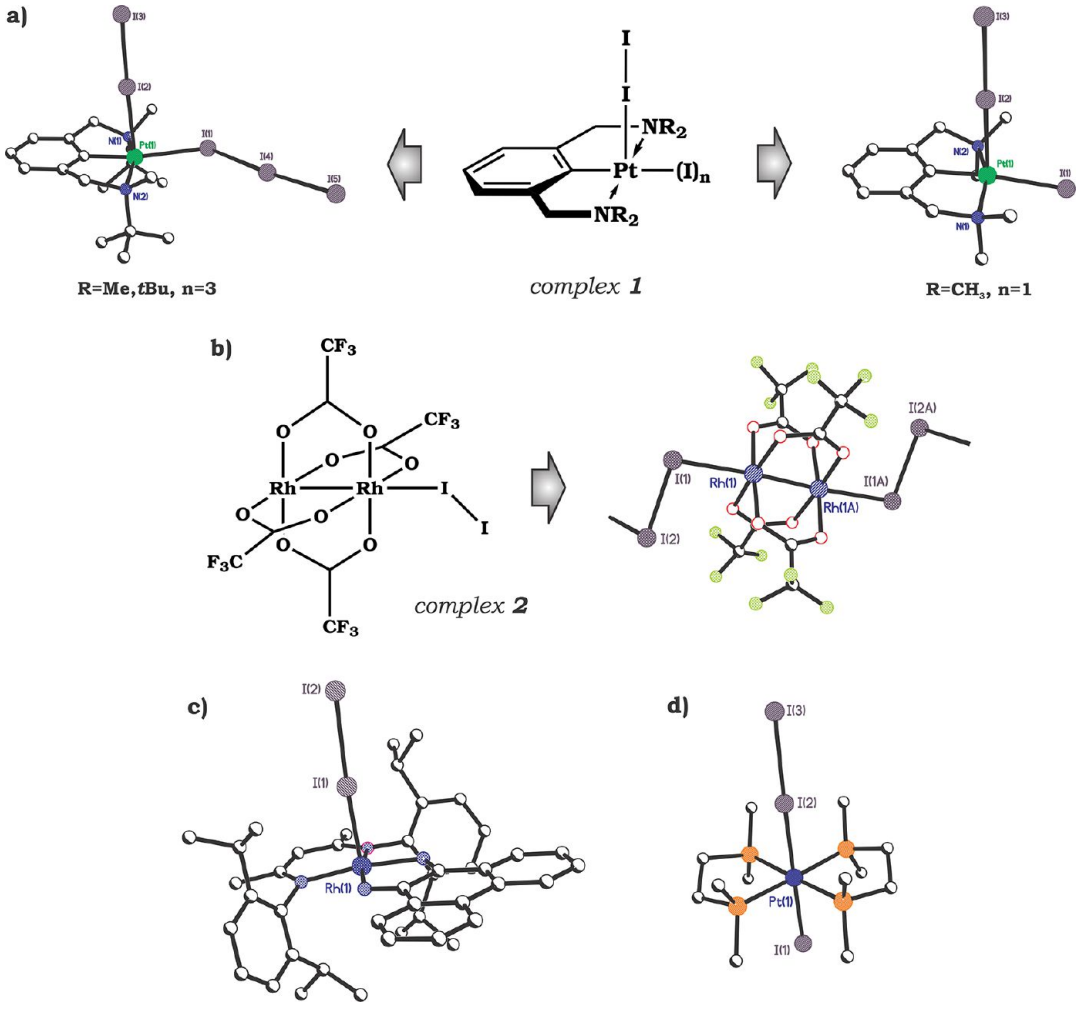

Figure 1. X-ray structures (hydrogen atoms are omitted for clarity) of adducts of I_2 investigated by (a) G. van Koten et al.,[2] complex **1**, (b) F. A. Cotton et al.,[3] complex **2**, (c) D. W. Shaffer et al.,[4] and (d) R. Makiura et al.[5] (cationic species, counterion not shown). For compounds in (a) and (b), ChemDraw schematic representations are also given.

Scheme 1

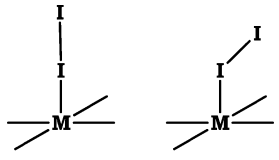

orbital, and one would expect bent "end-on" coordination of I_2 (Scheme 1B), as one finds in the (also rare) molecular I_2 complex of Cotton et al.[3] (Figure 1b), a coordination mode to which we will return.

In this Article, we explore the Janus-faced bonding of diiodine in some detail.[10] We also go on to what we hope are realistic predictions for enlarging the rare class of I_2 complexes acting either as donors or as acceptors.

RESULTS AND DISCUSSION

Reproducing the Structures. *Iodine as an Acceptor.* Geometry optimization of model complexes $[L(Y)Pt{\cdot}I_2]$ (Y = CH_3, F, Cl, Br, I; L = the simplified tridentate pincer ligand, real substituents at N replaced by hydrogens), followed by harmonic frequency calculations, revealed that all of these compounds correspond to minima on their potential energy surfaces (PES). Calculated geometrical parameters agree well with available experimental data[2] (Table 1; the results for Y = F, Cl, Br are given in the Supporting Information).

In all cases, the fifth axial ligand, I_2, is in linear "end-on" coordination mode with angle ∠C(or N)−Pt−I ≈ 90°. As one might expect, the I−I bond is substantially elongated in these adducts by comparison with unperturbed I_2. Furthermore, the

Table 1. Selected Calculated Geometrical Parameters of $[L(Y)Pt{\cdot}I_2]$[a]

				$[L^{Me}(I)Pt{\cdot}I_2]$	
parameter	I_2	Y = CH_3	Y = I	exp.[2]	calc.
Pt−I		2.84	2.90	2.895(1)	2.90
Pt−Y		2.13	2.70	2.727(1)	2.73
Pt−C		1.97	1.93	1.93(1)	1.93
Pt−N(1)		2.06	2.06	2.115(8)	2.11
Pt−N(2)		2.06	2.06	2.105(8)	2.11
I−I	2.69	2.83	2.81	2.822(1)	2.82
∠C−Pt−I		96°	87°	84.0(3)°	84°
∠C−Pt−Y		176°	172°	172.4(3)°	170°

[a]Bond lengths are in angstroms; angles are in degrees.

dx.doi.org/10.1021/ja312584u | J. Am. Chem. Soc. 2013, 135, 3262−3275

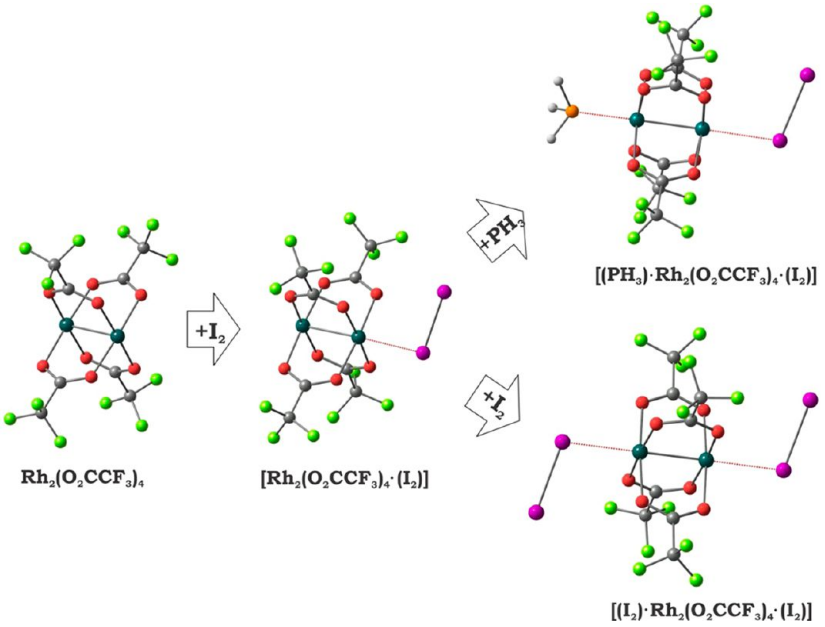

Figure 2. Equilibrium geometries for model compounds $[(Y)\cdot Rh_2(O_2CCF_3)_4\cdot(I_2)]$ (Y = □, I_2, PH_3) considered in this study.

Table 2. Selected Experimental and Calculated Geometrical Parameters of $[(Y)\cdot Rh_2(O_2CCF_3)_4\cdot(I_2)]$[a]

		$Rh_2(O_2CCF_3)_4$			$[(I_2)\cdot Rh_2(O_2CCF_3)_4\cdot(I_2)]$		
parameter	I_2	exp.	calc.	$[Rh_2(O_2CCF_3)_4\cdot(I_2)]$	exp.[b]	calc.	$[(PH_3)\cdot Rh_2(O_2CCF_3)_4\cdot(I_2)]$
Rh−Rh		2.3831(8)	2.38	2.41	2.415(1)	2.43	2.45
					2.417(1)		
Rh−I				2.79	2.8359(9)	2.84	2.90
					2.8239(9)		
I−I	2.69			2.69	2.7202(6)	2.69	2.69
Rh−Y					2.8359(9)	2.84	2.42
					2.8239(9)		
∠Rh−I−I				103°	95.31(2)°	102°	104°
∠O−Rh−I−I				42°	48.2(4)°	53°	43°

[a]Bond lengths are in angstroms; angles are in degrees. [b]For the experimental data, two values for bond lengths are provided because of the presence of two crystallographically independent dirhodium units in the unit cell. For angles, average values are presented.

shorter is the Pt−I bond length, the longer is the I−I distance. So, increasing coordination strength, as measured by the Pt−I bond length, results in decreasing strength of the I−I bond. We are assuming here a bond length−bond strength correlation, which has its limitations. The Pt−I bond length rises notably on going from Y = F to I (see the Supporting Information for details). In the case of Y = CH_3, this distance is shorter. The trend in Pt−Y bond length (see the Supporting Information for the full table) in general follows the covalent radii of the Y atoms. At the same time, the nature of Y influences only slightly the interaction between Pt(II) and pincer ligand L (Table 1).

Calculations with "real" ligands, carrying bulky substituents at N, have also been done (see the Supporting Information); they also give realistic geometries.

Iodine as a Donor. Geometry optimization of model complexes $[(Y)\cdot Rh_2(O_2CCF_3)_4\cdot(I_2)]$ (where Y = □, I_2, PH_3, Figure 2), followed by harmonic frequency calculations, indicated that all of these compounds correspond to minima on their PES. We looked at a range of Y ligands coordinated to the end of the $Rh_2(O_2CCF_3)_4$ entity not bound to I_2 because (a) such ligation might occur and (b) we wanted to see what might be its effect on I_2 bonding. Note that we do not try to model the infinite polymer as one observes in the crystal, but only discrete molecules. We do not think the polymerization is electronically or structurally significant (and provide below some evidence for this).

The calculated geometrical parameters agree well with available experimental data (Table 2).

In all cases, the axial I_2 ligand is in a bent "end-on" coordination mode with angle ∠Rh−I−I slightly greater than 100°. This geometry is in sharp contrast with what was found in the case of the van Koten compounds discussed above, where the fifth I_2 ligand approaches to the Pt(II) center in an "end-on" linear mode (∠M−I−I ≈ 180°), and, as our analysis will show, acts pretty much as an acceptor toward the metal fragment. At the same time, the bonding mode in $[(Y)\cdot Rh_2(O_2CCF_3)_4\cdot(I_2)]$ matches the expectations for maximized interaction between lone pair(s) of I_2 molecule (as a donor) and the available unoccupied σ^*-orbital of $Rh_2(O_2CCF_3)_4$ as an acceptor.

The constant value of the I−I bond length, 2.69 Å in isolated I_2 as well as in all adducts considered in this study, is interesting. Were the donation to $Rh_2(O_2CCF_3)_4$ entirely from π^* of I_2 (we will show this orbital below), we would expect a decrease in the I−I separation. Were the donation from both π

dx.doi.org/10.1021/ja312584u | J. Am. Chem. Soc. 2013, 135, 3262−3275

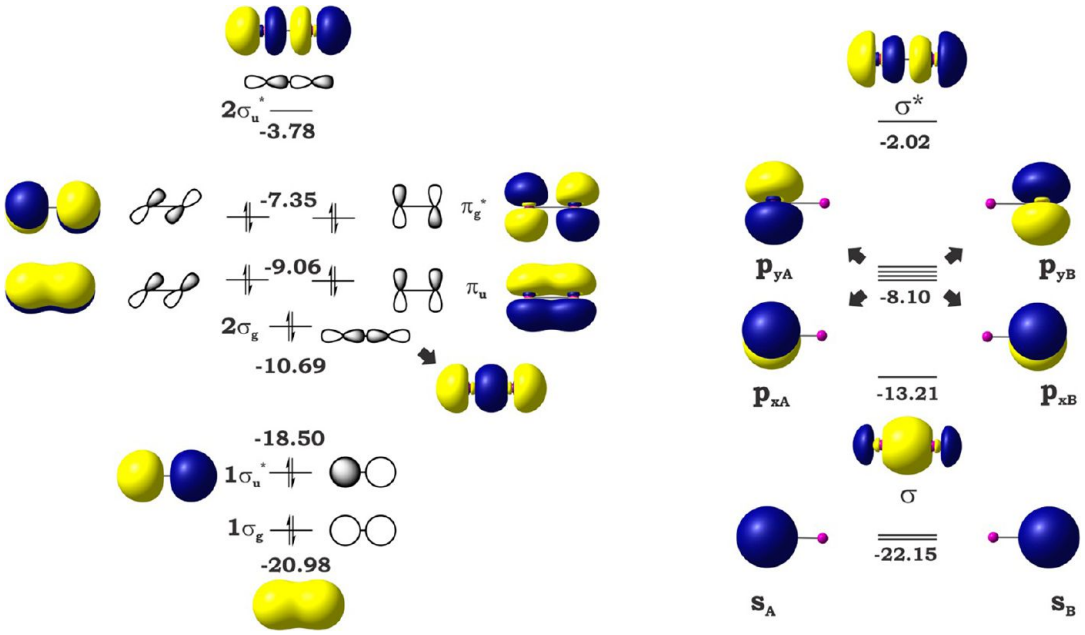

Figure 3. (left) The MO diagram for I_2. (right) Natural bond orbitals for the I_2 molecule. The energy levels (in eV) as well as orbital shapes come from calculations, but the energy scale is schematic.

and π^* of I_2 (they are not far in energy from each other), we would not expect much of a change in the I–I distance.

The Rh–Rh bond length is sensitive, in principle, to both types of electron transfer, from and to the metal fragment. In adducts of $Rh_2(O_2CCF_3)_4$ with I_2, the Rh–Rh bond is elongated by 0.04–0.09 Å relative to the unperturbed metal complex. Such an observation might indicate stronger donation from I_2 (to metal fragment σ^*, Rh–Rh antibonding) than the corresponding back-donation. However, it could also be that electron donation from the σ-orbital of the Rh_2-core to the acceptor σ^*-orbital of I_2 might be taking place, along with back-donation from the bonding σ-MO of diiodine to the σ^*-MO of the metal fragment. In both cases, an elongation of the Rh–Rh distance is expected.

Interestingly, the presence of the second axial ligand has some influence on such geometric parameters as the Rh–Rh and Rh–I bond length, but has no effect, as mentioned above, on the I–I bond. The trend observed from the two cases studied (PH_3 and I_2 as the second ligand) is that the stronger is the donor ability of the second axial ligand, the longer are these bonds. It appears that the presence of the second ligand weakens the Rh–I bond.

NBO Perturbation Theory. Theory reproducing the structures is a necessary beginning. Yet it tells precious little about the bonding. To get insight into the bonding, we carry out an analysis with natural bond orbital (NBO)[11] perturbation theory, as well and energy decomposition analysis (EDA).[12]

Within the NBO approach, one can choose different levels of localization. One choice is that of natural localized molecular orbitals (NLMO), which correspond to the first step in diagonalization of the density matrix (MO→NLMO). A Slater determinant of NLMOs is equivalent to the determinant of the wave function of the canonical MOs. The relationship between natural bond orbitals (NBO, the next step of diagonalization) and the corresponding NLMOs determines how well the chosen Lewis structure describes the electronic density of a given system. For all of the systems considered by us, the NBO description of a target orbital corresponds to >90% of a NLMO and, thus, can be used further to clarify the nature of the bonding.

The strength of donor–acceptor interactions between two fragments can be obtained within the NBO formalism by examining interactions between filled (*i*, donor) Lewis-type NBOs and empty (*j*, acceptor) non-Lewis NBOs.[11] Because these interactions lead to loss of occupancy of localized NBOs of an idealized Lewis structure to empty non-Lewis orbitals (and thus to deviation from an idealized Lewis structure description), they are referred to as delocalization corrections to the zeroth-order natural Lewis structure ($E^{(2)}_{i\rightarrow j}$).[11] We have found these to be a useful analytical tool.

The NBOs of a molecule are similar to and at the same time different from the canonical orbitals that the community is familiar with. We begin by comparing the two.

NBOs and Canonical MOs. The canonical orbitals of the I_2 molecule (Figure 3 left) are familiar. At low energy are the $1\sigma_g$ and $1\sigma_u$ orbitals, mainly 5s combinations. Above these, one finds the $2\sigma_g$, which normally is identified as a lone pair combination. Yet as Figure 3 shows, this orbital is also I–I σ-bonding; to put it another way, in the canonical molecular orbital picture, the σ-bonding in I_2 is distributed among the $1\sigma_g$ and $2\sigma_g$ orbitals.

Above the $1\sigma_g$ and $1\sigma_u$ orbitals are the π_u and π_g^*, containing between them 8 electrons. It makes sense to view these as the delocalized equivalent of localized lone pairs; the noded π_g^* is the HOMO. These canonical orbitals are split by 1.7 eV. The valence orbital set is completed by the LUMO $2\sigma_u^*$, the acceptor function of I_2.

If I_2 were to act simply as a donor, frontier orbital (or perturbation theory) thinking would lead one to think that interaction with π_g^* would be dominant. That would imply "bent" coordination, an L_nM–I–I angle perhaps somewhat greater than 90°, but certainly far from 180°.

The only way to get linear "end-on" coordination of I_2 would be to assume that the I_2 donor function is $2\sigma_g$. This seems energetically unlikely, but it needs to be considered as a possibility.

dx.doi.org/10.1021/ja312584u | J. Am. Chem. Soc. 2013, 135, 3262–3275

What about the potential acceptor behavior of I_2? The diiodine species has a relatively low-lying empty σ^*-orbital, $2\sigma_u$, made up of the antibonding combination of 5p orbital on each I. The electron affinity of I_2 is 2.524(5) eV.[13] This orbital is the reason I_2 tends to form very stable hypervalent anion I_3^- and, consequently, polyiodides.[14] Still another example of such bonding is in the known amine adduct $[(CH_3)_3N{\cdot}I_2]$.[15] The latter will be analyzed below in detail, serving as a model for axial acceptance by diiodine.

The NBOs of a molecule are in principle the best single configuration orbitals for a molecule. They resemble and yet may differ from the canonical orbitals of a molecule, which are more familiar to the community. NBOs often enhance localization in a chemically intuitive way, and when NBOs remain delocalized that is an informative signpost to an essential feature of the molecule.[11] I_2 is a good case in point; the NBOs are illustrated in Figure 3, right.

One is immediately struck by the localization, a localization that makes chemical sense. So the $1\sigma_g$ and $1\sigma_u$ canonical orbitals are replaced in the NBO analysis by two essentially pure, localized I 5s orbitals (s_A and s_B in Figure 3). Also, the four delocalized π_u and π_g^* MOs, which we anyway thought of as lone pair equivalents, emerge as exactly that −4 localized iodine lone pairs (p_{xA}, p_{yA}, p_{xB}, p_{yB}). The acceptor NBO of I_2 (σ^*) remains much as the canonical $2\sigma_u^*$, but the third NBO up in energy, (σ), while generally resembling the canonical $2\sigma_g$, has clearly concentrated into itself all of the σ bonding. Also, unlike $2\sigma_g$, σ has little "out-pointing" lone pair character.

We will show the NBOs of iodine's bonding partners in our detailed analysis of the molecule's interactions in compounds **1** and **2**. This we now proceed to do.

The Bonding of Iodine in the van Koten Compounds. We begin with the calculated electron distribution in model complexes, Figure 4.

The bonding energy (defined as $E_{adduct} - \sum(E_{fragments})$, negative when the molecule is more stable that the fragments) in these complexes is not large, −19 kcal/mol for Y = CH_3, −14 for Y = I. The Pt−I bond orders go along with this moderate bonding, increasing from Y = I (0.22) to Y = F (0.25, Supporting Information); for Y = CH_3, the bond order was found to be the largest (0.27). The variation is small overall. At the same time, the I−I bond index is substantially decreased (Figure 4) in comparison with that in an unperturbed I_2 molecule (1.03).

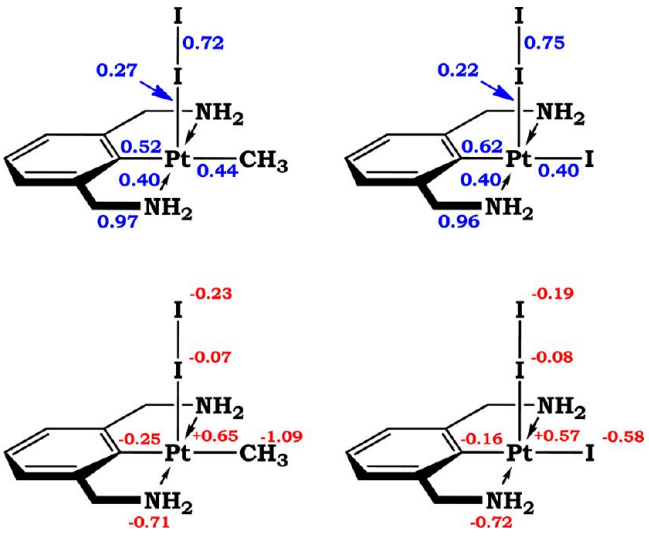

Figure 4. Wiberg bond orders and NBO charges for model complexes $[L(Y)Pt{\cdot}I_2]$, where Y = CH_3, I. Blue color is for bond orders, and red is for charges.

We saw the NBOs of iodine in Figure 3, at right. What are the NBOs of the pincer fragment that might interact with these? There are many such orbitals; important ones among these are shown in Figure 5, with occupied orbitals in the bottom and middle rows, and unoccupied (Lewis acid NBO, LAO) in the top row.

The figure shows nitrogen and Y ligand lone pairs (in the bottom row). The middle row shows the high energy occupied NBOs, four quite localized d orbitals on Pt. The d_z^2 (z axis is defined perpendicular to local quasi 4-fold coordination plane), the only suitable by symmetry for donation to σ^* of I_2, is at the left. Acceptor orbitals include a C−Pt σ^* with $d_{x^2-y^2}$ character, and an in-plane s−$d_{x^2-y^2}$ hybrid.

The outcome of an NBO perturbation analysis is given in Table 3.

The NBO analysis (Table 3) shows that the M→(I_2) term (I_2 acting as acceptor) clearly dominates over the (I_2)→M one (I_2 acting as donor) in all model complexes. There are three components of the M→(I_2) contribution (see the Supporting Information for details), but the major one is from d_z^2(Pt) to σ^*(I−I) (see Figure 6 for a graphical representation of the NBOs involved). The largest value of this interaction was found for Y = CH_3, which agrees with trends observed in distances and bond orders, as well as in total bonding energy (Table 2 and Supporting Information). Note that the NBO orbitals involved are very localized (d_z^2 on Pt) and for I_2 slightly asymmetrical relative to either the canonical MO's in Figure 3 (left) or the σ^* in Figure 3 (right).

As Table 3 shows, there is a minor contribution from (I_2)→M donation, constituting ∼15% of the total attraction between I_2 and metal fragment, as estimated by $E^{(2)}$. The largest component of I_2 donation is electron transfer from the s-type lone pair (s_A in Figure 5) of the iodine atom in Table 3. The acceptance here is by an empty metal-based NBO (LAO(Pt) in Table 3), which has Pt s and d character (∼80% of s-character, see Figure 7, right). There is no trace of involvement of the p_z orbital of the Pt(II) in bonding with the axial ligand.

For comparison, a similar analysis of interactions between the nitrogen atoms of the pincer ligand, or the in-plane coordinated Y group, and Pt(II) was carried out (also indicated in Table 3, and illustrated in Figure 8). The contrast with the axial bonding to I_2 is striking. In both instances, the in-plane bonding is dominated by ligand→M or classical donor contributions. We do not analyze in detail the special localization of the NBOs on Pt and the ligands, but it is clear that the ligand donor orbitals are quite different from the canonical, symmetry-adapted orbitals of the molecule; they are localized lone pairs on the individual N atoms (N(1) and N(2)) and on Y. The acceptor orbitals on the metal are LAO(Pt) (Figure 7, right) and an orbital partially localized on Pt (containing $d_{x^2-y^2}$ character there), but also strongly involved in antibonding to the phenyl carbon (see the top right image in Figure 8). We call this orbital σ^*(C−Pt). It should be noted these interactions are significantly stronger than that between the metal fragment and I_2.

We note here an XPS study of the van Koten compounds in which some depletion of electron density at the Pt is found, while retaining a Pt(II) formal oxidation state.[16] In our

dx.doi.org/10.1021/ja312584u | J. Am. Chem. Soc. 2013, 135, 3262−3275

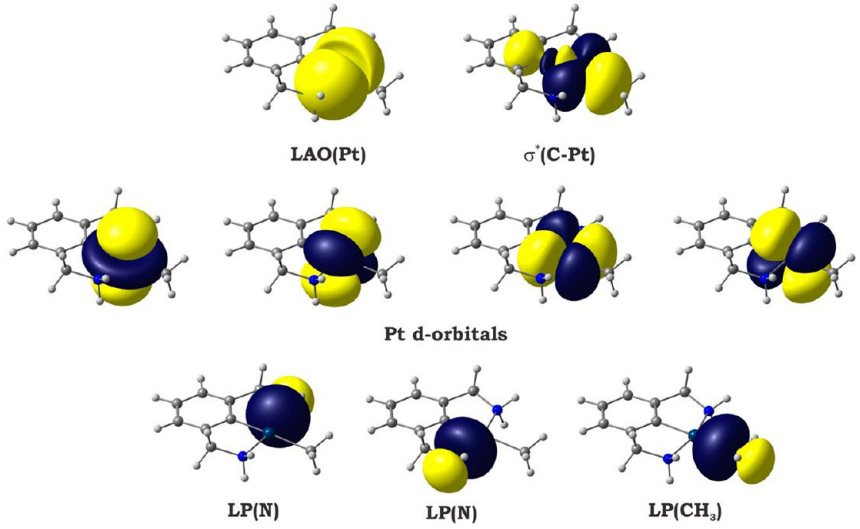

Figure 5. Selected NBOs of van Koten metal fragment [L(CH$_3$)Pt].

Table 3. Results of NBO Analysis of Donor−Acceptor Interactions in [L(Y)Pt·I$_2$] Adducts, Estimated by Second-Order Perturbation Theory, $E^{(2)}_{i\rightarrow j}$ (in kcal/mol, PBE0/TZVP/ZORA)

parameter	Y = CH$_3$	Y = I
	M^a→I$_2$	
σ(C−Pt)→σ*(I−I)	4	5
d$_z^2$(Pt)→σ*(I−I)	30	22
d$_z^2$(Pt)→5d(I)	4	3
	I$_2$→M^a	
σ(I−I)→LAO(Pt)^b	1.4	1.2
LP(I)^b→LAO(Pt)^b	5.4	4.9
	Y→M^a	
LP(1)(Y)^b→LAO(Pt)^b	163	111
LP(1)(Y)^b→σ*(C−Pt)	156	87
	N^c→M^a	
LP(N(1))^b→LAO(Pt)^b	135	146
LP(N(1))^b→σ*(C−Pt)	18	28
LP(N(2))^b→LAO(Pt)^b	133	146
LP(N(2))^b→σ*(C−Pt)	19	28
$-D_e$^{d}	−19	−14

^{a}M designates the metal fragment. ^{b}LP is the localized lone pair of the donor atom (different for each donor, see Figures 5−8); Y is the fourth in-plane ligand at Pt. LAO(Pt) designates the available empty (Lewis acceptor) orbital of the Pt(II) center. ^{c}N(1) and N(2) represent nitrogen atoms in the pincer ligand. ^{d}$-D_e$ (bonding energy) = $E_{adduct} - \sum(E_{fragments})$, where E_{adduct} and $E_{fragment}$ are total (PBE0/TZVP) energies of adducts and separately optimized fragment, respectively. D_e is positive, and $-D_e$ negative when the molecule is more stable than the fragments.

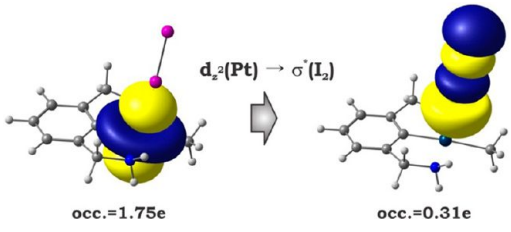

Figure 6. The major contributor to the M→(I$_2$) interaction in an NBO analysis (for Y = CH$_3$).

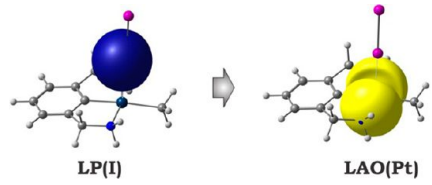

Figure 7. The major contributor to the (I$_2$)→M interaction in an NBO analysis (for Y = CH$_3$).

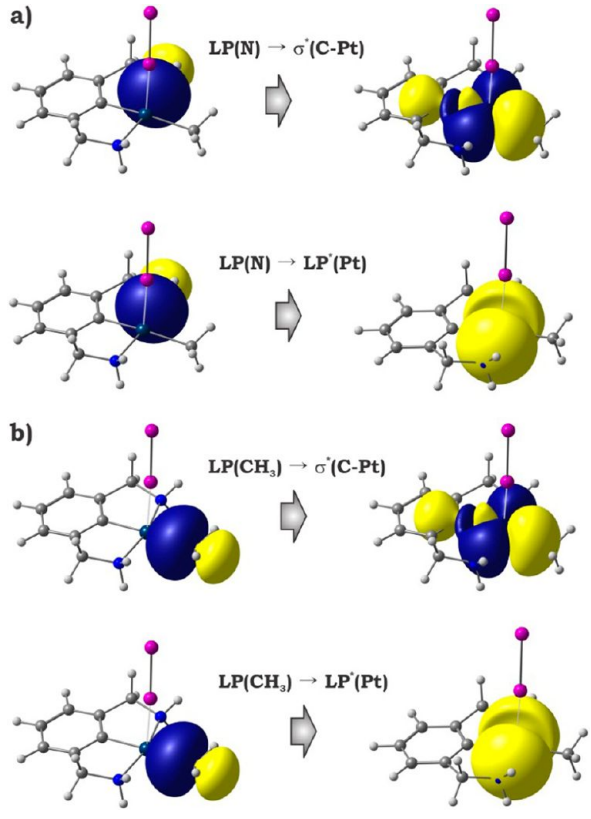

Figure 8. N→M (a) and Y→M (b) interactions in the NBO analysis (for Y = CH$_3$).

dx.doi.org/10.1021/ja312584u | J. Am. Chem. Soc. 2013, 135, 3262−3275

calculations, the Pt d_z^2 occupation goes from 2.00*e* to 1.75*e* in I_2 bonding.

The NBO analysis of the electronic structure of our model compounds showed a relatively small influence of charge on the metal center on the bonding to I_2. Could this be indicative of a greater importance of the covalent term (here, donor−acceptor) over the electrostatic one in bonding? Covalent and electrostatic contributions as well as repulsive interactions are conveniently separated in an EDA analysis. The results of such a study are detailed in Table 4.

Table 4. Results of EDA Analysis of Bonding in $[L(Y)Pt{\cdot}I_2]$ Adducts (in kcal/mol, PBE0/TZ2P/ZORA)

parameter	Y = CH_3	Y = I
ΔE_{int}	−20	−15
ΔE_{orb}	−38 (45%)	−32 (45%)
ΔE_{elstat}	−48 (55%)	−39 (55%)
ΔE_{Pauli}	+66	+56
$-D_e$	−17	−12
ΔE_{prep}	+3	+3

The EDA analysis unambiguously shows the importance of contributions of both types (Table 4). For all compounds considered, ΔE_{orb} (usually thought of as the describing the covalent or donor−acceptor part of bonding) is by ca. 10 kcal/mol lower than ΔE_{elstat}, a measure of the electrostatic or the ionic contribution. The interplay between these two kinds of bonding is essentially the same through the entire series (ΔE_{orb}:ΔE_{elstat} = 45%:55%). The repulsive interactions, estimated here by the Pauli repulsion term (ΔE_{Pauli}), are relatively high (Table 4), decreasing slightly from R = CH_3 (+66 kcal/mol) to Y = I (+56 kcal/mol). The calculated bonding energy ($-D_e$) falls somewhat, from −17 kcal/mol for Y = CH_3 to −12 kcal/mol for Y = I, as does ΔE_{int}. Thus, the bonding of I_2 to the metal fragment is not very strong, as we already knew from direct calculations described above.

Experimentally, the I−I bond length in the van Koten compounds lengthens relative to the free molecule. Theory is in accord (Table 1), and the Wiberg bond order (Figure 4) indicates substantial weakening of the I−I bond. Preliminary calculations for Br_2 and Cl_2 complexes indicate that the X−X bonds are weakened still further in these. Such complexes are likely to go on to an oxidative addition, to Pt(IV) octahedral complexes. This is in fact observed experimentally.[17] Interestingly, all attempts to localize similar complexes for F_2 resulted in *cis*-difluoro compound of Pt(IV). This might be considered as an oxidative addition reaction with an unobserved intermediate or transition state corresponding to a donor−acceptor adduct with difluorine.

Van Koten and co-workers, indeed, suggested that the axial I_2 in **1** bonds not as a donor, but as an acceptor. Synthesis was followed by theoretical modeling by Bickelhaupt, Baerends, and Ravenek.[18] In their study, the interaction between a model $PtCl_4^{2-}$ metal fragment and difluorine (F_2) was investigated. The authors concluded that the F_2 ligand, occupying the axial position, most probably behaves as electron acceptor rather than electron donor. Constrained calculations with I_2 as an axial ligand supported their conclusions.

We will return to further experimental evidence for the bonding the NBO picture shows, but let us first show the great

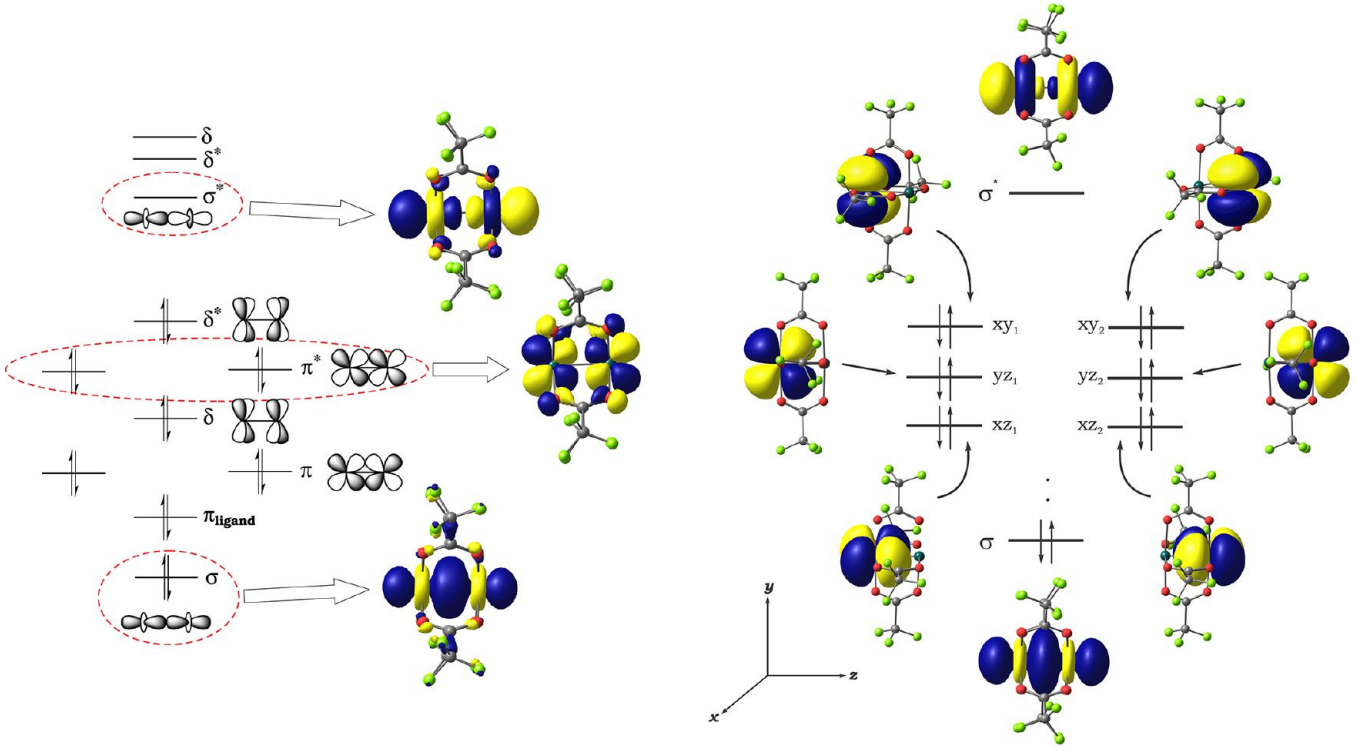

Figure 9. (left) Schematic MO picture for the metal−metal bonded paddle-wheel dirhodium tetracarboxylate, $Rh_2(O_2CR)_4$. The molecular orbitals discussed in the text are highlighted by insets. (right) Selected natural bond orbitals for the $Rh_2(O_2CCF_3)_4$ complex. Other orbitals come in energy between σ(Rh−Rh) and π(Rh−Rh), but are omitted for clarity. Subscripts 1 and 2 refer to the left and right Rh, respectively. The *xy*, *yz*, *xz* orbitals are at the same energy; they are separated for clarity.

dx.doi.org/10.1021/ja312584u | *J. Am. Chem. Soc.* 2013, 135, 3262−3275

Table 5. Donor–Acceptor Interactions in $[(Y)\cdot Rh_2(O_2CCF_3)_4\cdot(I_2)]$ Adducts (Where Y = □, I_2, PH_3), Estimated by the Second-Order NBO Perturbation Theory, $E^{(2)}_{i\rightarrow j}$ (in kcal/mol, PBE0/TZVP/ZORA)

	$E^{(2)}_{i\rightarrow j}$			
parameter	$[Rh_2(O_2CCF_3)_4\cdot(I_2)]$	$[(I_2)\cdot Rh_2(O_2CCF_3)_4\cdot(I_2)]$	$[(PH_3)\cdot Rh_2(O_2CCF_3)_4\cdot(I_2)]$	$[(PH_3)\cdot Rh_2(O_2CCF_3)_4]$
		$(I_2)\rightarrow(Rh_2)^a$		
$LP_1(I_2)^b\rightarrow\sigma^*$(Rh–Rh)	43	34	29	
$LP_2(I_2)^b\rightarrow\sigma^*$(Rh–Rh)	5	4	3	
		$(PH_3)\rightarrow(Rh_2)^a$		
$LP(PH_3)^b\rightarrow\sigma^*$(Rh–Rh)			82	93

$^a(Rh_2)$ hereafter designates the metal fragment. ^{b}LP is the localized lone pair of the donor atom (different for each donor).

contrast of the bonding picture just analyzed with what happens in the paddle-wheel complex **2**.

The Canonical Orbitals and NBOs of $Rh_2(O_2CCF_3)_4$. The metal–metal bonding in dirhodium(II,II) tetracarboxylates ($Rh_2(O_2CR)_4$) is well-understood. It is generally accepted that the formal metal–metal bond order in such compounds is 1. In a simplified molecular orbital picture of the Rh_2^{4+} core (Figure 9 left), 8 of the 14 valence electrons are distributed in mainly metal 4d-based σ-, π-, and one δ-orbital, whereas the remaining 6 electrons occupy the π^*- and δ^*-orbitals. The two other δ orbital on the metals are pushed to high energy by Rh–carboxylate σ-bonding. The lowest unoccupied MO of the system is clearly identified as a metal–metal antibonding σ^*-orbital.

Because of the presence and relatively low energy of this σ^*-orbital, $Rh_2(O_2CR)_4$ behaves as a Lewis acid toward donor organic molecules, which then electronically (and sterically) are expected to coordinate along the Rh–Rh axis. This reactivity is most pronounced in the case of fully fluorinated trifluoroacetate ligands ($Rh_2(O_2CCF_3)_4$, taken as the model in this study), which can even form stable adducts with such relatively weak donors as planar and curved polyaromatic molecules.[19] Another feature of these systems is the presence of relatively high-lying π^* and δ^* orbitals that could potentially act as π-donors, available for back-donation in axial bonding.

NBO localization (or lack of it) makes chemical sense for $Rh_2(O_2CCF_3)_4$, as it did for I_2. The π, π^* and δ, δ^* canonical delocalized molecular orbitals of the paddle-wheel complex are replaced by a set of six essentially pure 4d orbitals, which are localized on corresponding Rh atoms of the Rh_2-core (Figure 9, right). The acceptor antibonding NBO of dirhodium core (σ^*) as well as its low-energy bonding partner remain much as the corresponding canonical MOs (Figure 9, left). These localized and delocalized NBOs will be used further in the perturbation analysis.

One last remark is needed before we proceed to the analysis of interactions. Please take a look at the NBOs of I_2 and those of the paddle-wheel complex. Except for the δ orbitals, the NBOs of the two systems are very similar; note especially the shapes of the σ and σ^* orbitals. In a way, I_2 and $Rh_2(O_2CCF_3)_4$ are isolobal; we will explore this unexpected similarity in a future paper.

The Nature of the $Rh_2(O_2CCF_3)_4$–I_2 Bonding. The dominant donor–acceptor interactions emerging from the NBO analysis are collected in Table 5.

The NBO Analysis Clearly Reveals That the Bonding between $Rh_2(O_2CCF_3)_4$ and I_2 Is Dominated by the Dimetal Fragment Acting as an Acceptor and I_2 as a Donor. In contrast to the van Koten complexes investigated above, the $(Rh_2)\rightarrow(I_2)$ contribution was found here to be tiny, ~1 kcal/mol for all adducts considered. The major component of the $(I_2)\rightarrow(Rh_2)$ bonding in the present case derives from electron donation by a p-type lone pair of I_2 to the antibonding Rh–Rh σ^* orbital, located on the dirhodium core (see Figure 10 for a graphical representation of the NBO's involved). Note that the donor orbital ($LP_1(I_2)$ here) is slightly polarized toward the acceptor center, a typical feature of the NBO analysis, which forms NBOs for the composite molecule that may differ slightly from the NBOs of an isolated, noninteracting fragment.

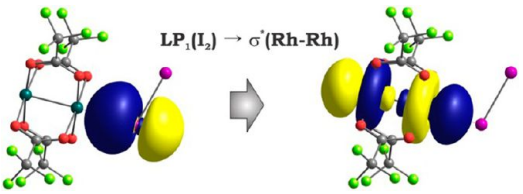

Figure 10. The major contributor to the $(I_2)\rightarrow(Rh_2)$ interaction in an NBO analysis (for $[Rh_2(O_2CCF_3)_4\cdot(I_2)]$).

Additionally, there is a small donor contribution from another (s-type) lone pair of the same iodine (labeled $LP_2(I_2)$). However, due to a substantial energy difference between interacting donor and acceptor orbitals, this interaction is weak and does not appear to be larger than 5 kcal/mol (Figure 11, Table 5). Interestingly, such a donor orbital of the I_2 was responsible for the small $(I_2)\rightarrow$M donor–acceptor interaction in van Koten's complexes.

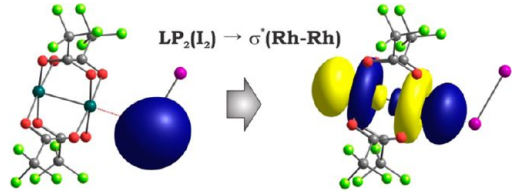

Figure 11. The minor contributor to the $(I_2)\rightarrow(Rh_2)$ interaction in an NBO analysis (for $[Rh_2(O_2CCF_3)_4\cdot(I_2)]$).

The donor–acceptor interaction between the Rh_2-core and I_2 decreases in the presence of a second axial ligand (Table 5). The trend observed is that the stronger of a donor is the second axial ligand, the weaker is the I_2 molecule bound to the metal. This finding correlates well with the nature of interactions between axial ligand(s) and the paddle-wheel dirhodium(II,II) complex; both ligands are donating to the same acceptor orbital (σ^*(Rh–Rh) here).

For comparison, a similar analysis of interactions between a phosphine ligand (as an example of a good donor) and the Rh_2-core was also carried out (Table 5, Figure 12). The nature of Rh–P bonding was found to be dominated by interaction

dx.doi.org/10.1021/ja312584u | J. Am. Chem. Soc. 2013, 135, 3262–3275

Table 6. EDA Analysis of Bonding in $[(Y)\cdot Rh_2(O_2CCF_3)_4\cdot(I_2)]$ Adducts (Where Y = □, I_2, PH_3)[a]

	$[(Y)\cdot Rh_2(O_2CCF_3)_4\cdot(I_2)]$				
parameter	Y = □[b]	Y = I_2[b]	Y = PH_3[b]	Y = PH_3[c]	$[(PH_3)\cdot Rh_2(O_2CCF_3)_4]$[c]
ΔE_{int}	−14	−10	−8	−24	−30
ΔE_{orb}	−25 (44%)	−21 (42%)	−16 (38%)	−41 (33%)	−48 (35%)
ΔE_{elstat}	−32 (56%)	−29 (58%)	−26 (62%)	−83 (67%)	−90 (65%)
ΔE_{Pauli}	+44	+40	+34	+99	+108
$-D_e$[d]	−12	−9	−7	−21	−26
ΔE_{prep}	+1	+1	+1	+3	+4

[a]The percentages are the contributions of the respective terms to the sum of $\Delta E_{orb} + \Delta E_{elstat}$ (PBE0/TZ2P/ZORA). [b]Analysis was performed for the Rh−I bond. [c]Analysis was performed for the Rh−P bond. [d]$-D_e = E$(molecule) − E(fragments); negative for bound molecule.

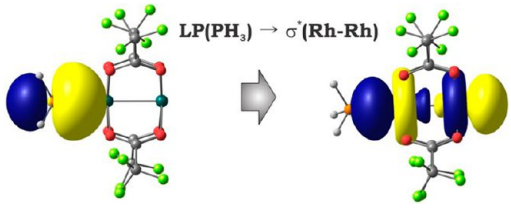

Figure 12. The major contributor to the $(PH_3)\rightarrow(Rh_2)$ interaction (for $[Rh_2(O_2CCF_3)_4\cdot(PH_3)]$).

between the phosphorus-based lone pair of PH_3 (a donor) and the σ^* orbital of the Rh_2-core (an acceptor). Yet the strength of the donor−acceptor interaction is much higher than for I_2 (Table 5). This finding agrees with the greater total bonding energy of the Rh−P bond discussed above.

The interplay between covalent and electrostatic components of bonding can be clarified by an EDA analysis, Table 6.[12]

As in compounds in which I_2 acts as an acceptor, ΔE_{orb} and ΔE_{elstat} for the Rh−I bonding are both important. ΔE_{orb} (usually associated with covalent or donor−acceptor bonding) is by ∼8 kcal/mol smaller in magnitude (both are negative) than ΔE_{elstat}, a measure of the ionic or electrostatic component. The relationship between donor−acceptor and electrostatic contributions is not constant and depends on the donor ability of the second axial ligand (Table 6). The absolute values of both ΔE_{elstat} and ΔE_{orb} contributions to Rh−I bonding decrease smoothly with increasing donor ability of the second axial ligand Y. The same trend was found for the Rh−P bond (Table 6), albeit the total bonding is much stronger than for the Rh−I bond.

The repulsive interactions, estimated by the Pauli repulsion term (ΔE_{Pauli}), are consistently high, decreasing from Y = □ (+44 kcal/mol) to Y = PH_3 (+34 kcal/mol). The bonding energy ($-D_e$, negative for a bound molecule) follows the ΔE_{orb} trend, decreasing in magnitude somewhat from −12 kcal/mol (without the second axial ligand) to −7 kcal/mol (for Y═ PH_3).

We think the main reason for the relative weakness of the metal−I_2 bonding, the small magnitude of $-D_e$, is due to just the repulsive interactions coming out of the EDA analysis. Otherwise, it would be difficult to reconcile the high donor−acceptor bonding stabilizations of the perturbation analysis (Table 5) with the low total bonding energy.

We have now finished the analysis of the bonding in both kinds of complexes; the contrast is stark: I_2 is an acceptor in complex **1**, and just as clearly a donor in complex **2**. We seek further support in some model compounds.

Further Experimental Evidence for Donor−Acceptor Bonding in the van Koten Compounds. We mentioned at the outset the similarity between the case we are making in this Article for I_2 acting as an acceptor and/or a donor and an analogous situation for SO_2 as a ligand. In fact, van Koten and co-workers have prepared SO_2 complexes of $[L^{Me}(I,Cl)Pt]$.[20] Also, the SO_2 ligand is "inclined"; that is, the plane of the coordinated SO_2 is closer to the [L(Y)Pt] plane than perpendicular to it. This is similar to the geometry of the Rh(I) and Ir(I) ML_4 complexes, in which the SO_2 acceptor capability was displayed.[9]

The van Koten group has also found good evidence for donor function in the Pt d_z^2, by the formation of $Pt^-\cdots H-N^+$ hydrogen bonds.[21]

Models for Donation/Acceptance. Is the donor behavior of an [L(Y)Pt] metal fragment toward I_2 that we found specific for this type of (pincer) ligand? We do not think so; we are able to establish similar bonding (see the Supporting Information) in a model square-planar d^8 Pt(II) compound of a rather different type, a simple $[(CH_3)_2(PH_3)_2Pt]$ model (Scheme 2, right) and its adduct with I_2 (Figure 13).

We also probed the bonding of our model d^8 square-planar Pt(II) complex (with Y = I) toward ligands that can (or we think they can) show only one type of coordination mode, donor or acceptor. NH_3 and BH_3 are the obvious choices, if we try to avoid charge and effects of π-donation or acceptance.

When we replaced the I_2 fragment in $[L(I)Pt\cdot(I_2)]$ by NH_3 and allowed the geometry of the complex to relax, the NH_3 donor ligand did not stay at axial position, but left its original

Scheme 2

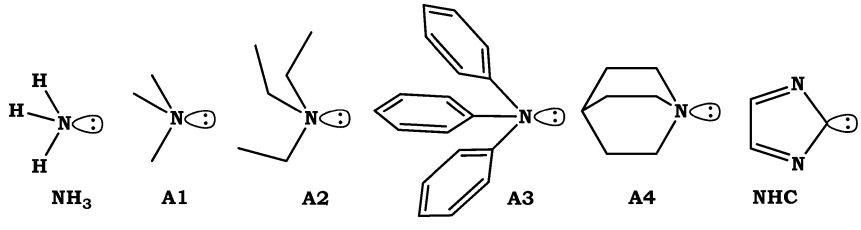

dx.doi.org/10.1021/ja312584u | J. Am. Chem. Soc. 2013, 135, 3262−3275

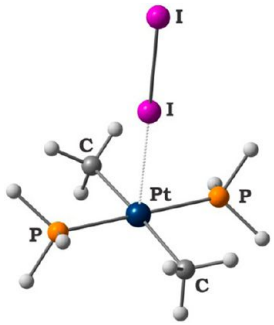

Figure 13. Equilibrium geometry configuration of the model adduct $[(CH_3)_2(PH_3)_2Pt{\cdot}I_2]$.

coordination place. Eventually, the geometry optimization process converged to a structure in which the NH_3 ligand is weakly bound (hydrogen bonding?) to one of the two hydrogen atoms of an amino group of the pincer ligand.

We turned next to a ligand that has little option but to be an acceptor, BH_3. Actually, the I_2 molecule might be a better acceptor, judging by the position of its LUMO (−3.78 eV), while that of BH_3 is −1.95 eV. Yet clearly BH_3 is a relatively strong Lewis acid. Geometry optimization converged to the stable structure of a $[L(I)Pt{\cdot}(BH_3)]$ adduct, where the BH_3 ligand occupies the fifth axial position (with Pt−B bond length of 2.27 Å, Figure 14). An NBO and EDA analysis (see the

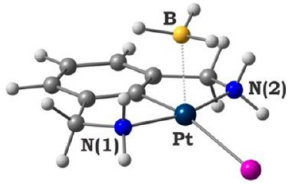

Figure 14. Equilibrium geometry for the adduct $[L(I)Pt{\cdot}(BH_3)]$.

Supporting Information) confirms the acceptance of the BH_3 moiety through its p_z orbital. With a bonding energy of −17 kcal/mol, this might be a complex that could be made.

Adducts of I_2 with Pure Organic Donors. We have now good theoretical evidence for I_2 bonding as an acceptor in the van Koten compounds. As still another link in establishing this unusual bonding, we probed the acceptor bonding capability of I_2 with organic donors (Scheme 2). Such adducts with amines are known experimentally, and their linear coordination mode is established.[15,22] For the sake of comparison, analogous adducts of BH_3 were also considered theoretically. The specific adducts calculated include ammonia (NH_3), trimethylamine (**A1**), triethylamine (**A2**), triphenylamine (**A3**), azabicyclooctane (**A4**), and the parent *N*-heterocyclic carbene (**NHC**) (Scheme 2). Geometrical configurations for two of these are presented in Figure 15; the others are discussed in the Supporting Information, where an NBO and EDA analysis of the bonding is given in some detail. Interestingly, a new kind of interaction, which includes the 5d orbital of diiodine as LAO, is notably large in the case of NHC, whereas for amine adducts it was found to be almost negligible.

The known linear coordination mode of the I_2 moiety (in $[(N(CH_3)_3){\cdot}(I_2)]$) is well reproduced in all optimized equilibrium geometries (Figure 14a). The trends in distances between the two interacting fragments are very similar for I_2 and BH_3 adducts, supporting our view that I_2 in these adducts

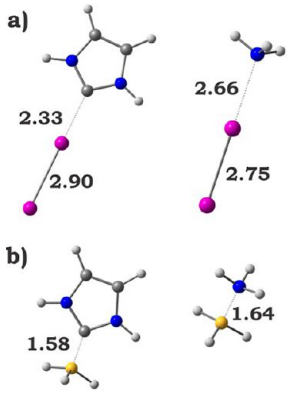

Figure 15. Equilibrium geometrical configurations of adducts of (a) I_2 and (b) BH_3 molecules with organic donor molecules (exemplified by **NHC** and **A1** molecules), with selected bond lengths (in angstroms).

with a N lone pair behaves as an acceptor rather than a donor. The calculated bonding energies ($-D_e$) range from −0.5 kcal/mol for $[(\mathbf{A3}){\cdot}(I_2)]$ to −23 kcal/mol $[(NHC){\cdot}(I_2)]$ for I_2-based adducts, and from −12 kcal/mol for $[(\mathbf{A3}){\cdot}(BH_3)]$ to −60 kcal/mol for $[(NHC){\cdot}(BH_3)]$ for BH_3-derivatives.

Adducts of I_2 with Model Acceptors. Might the donor behavior of I_2 also emerge in bonding with other molecules, for instance, clear organic and/or inorganic acceptors, such as H^+, $AlCl_3$, and $B(CF_3)_3$? We investigated such complexes; geometrical configurations of all adducts are presented in Figure 16 together with selected geometrical parameters. A vibrational analysis indicates that all three complexes are stable.

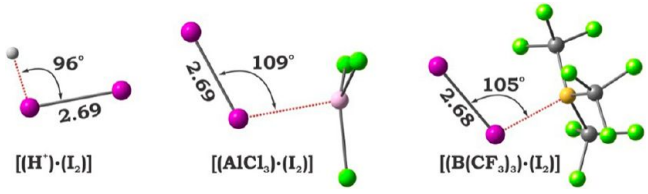

Figure 16. Equilibrium configurations of adducts of I_2 with organic/inorganic acceptor molecules, along with selected geometrical parameters.

In all adducts studied here, one sees clearly a bent coordination mode of the I_2 moiety (with ∠I−I−E from 96° for E = H to 109° for E = Al), in concord with what was experimentally found for the $Rh_2(O_2CCF_3)_4$ complex. Interestingly, the I−I bond length remains essentially the same through all of the series and is equal to that in unperturbed I_2 molecule (Table 1). This finding is consistent with the donor behavior of I_2, and participation of both π and π^* lone pairs of this molecule (in a canonical MO viewpoint) in electron donation to the acceptor (H^+, $AlCl_3$, and $B(CF_3)_3$). We also find substantial bonding for the simple BH_3 adduct of I_2. Experimental efforts at making this species are underway; a full discussion of the bonding in $[(BH_3){\cdot}(I_2)]$ and energetics will eventually be made in conjunction with experimental work.

Although we have found that I_2 forms an adduct with simple organic/inorganic acceptors, how stable are they? Also, are they different from what we found in the case of metal complexes? Protonation of diiodine is a highly exothermic process; the proton affinity of I_2 calculated by us is 156 kcal/mol. There appears to be no value in the literature for this heat of formation. One could compare other proton affinities of NH_3

dx.doi.org/10.1021/ja312584u | *J. Am. Chem. Soc.* 2013, 135, 3262−3275

(214 kcal/mol) and H_2O (174 kcal/mol), calculated at the same level of theory.[23]

Estimations of the bonding energy show a value of −16 kcal/mol for $[(B(CF_3)_3)\cdot(I_2)]$, almost twice as large as that for $[(AlCl_3)\cdot(I_2)]$ (−9 kcal/mol). This bond strength is of the same magnitude as that in the organometallic adducts $[Rh_2(O_2CCF_3)_4\cdot(I_2)]$ (−13 kcal/mol) and $[(I_2)\cdot Rh_2(O_2CCF_3)_4\cdot(I_2)]$ (−10 kcal/mol) considered above. An EDA analysis provided an explanation of the higher stability of $[(B(CF_3)_3)\cdot(I_2)]$ in comparison with $[(AlCl_3)\cdot(I_2)]$ (see the Supporting Information).

An Adduct of I_2 with I_2. Given that I_2 can act as a donor and as an acceptor in organometallic complexes, the following question arises quite naturally: Can diiodine interact with itself, one molecule acting as a donor and another as an acceptor? We looked at a hypothetical $[(I_2)\cdot(I_2)]$. Such an adduct indeed corresponds to a minimum on its PES, as supported by a vibrational analysis. The bonding energy, to which we will return, is small, −3 kcal/mol. Selected geometrical features as well as NBO parameters are presented in Figure 17.

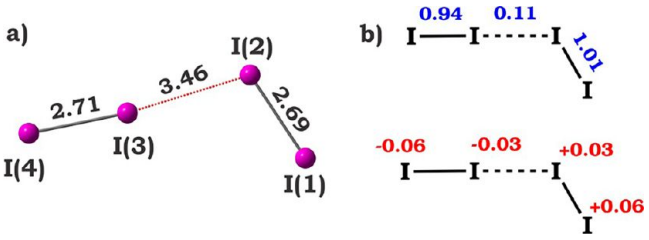

Figure 17. Equilibrium geometry configuration along with selected (a) geometrical parameters and (b) Wiberg bond orders (blue) and NBO charges (red) for the adduct $[(I_2)\cdot(I_2)]$.

The coordination mode is bent ($\angle$I(1)−I(2)−I(3) = 106°) for one I_2-moiety and near linear ($\angle$I(2)−I(3)−I(4) = 174°) for another. By now, the association of geometry with donor−acceptor character should be obvious; one presumes the first I_2-fragment (I(1)−I(2)) to be a donor, and the second one (I(3)−I(4)) to be an acceptor. In the donor part of the dimer, the I−I bond length remains the same as in an unperturbed I_2 molecule (2.69 Å), while in the acceptor part this bond is slightly elongated (Δd(I−I) = 0.03 Å). The small elongation and relatively large distance between interacting fragments is consistent with the low stability of the adduct, −3 kcal/mol, as mentioned. The NBO and EDA analyses (see the Supporting Information) are consistent with the donor−acceptor bonding.

The first reaction to −3 kcal/mol bonding energy of a dimer of two iodine molecules is that (a) this is probably a dispersion energy, and (b) a quadrupole−quadrupole interaction might be responsible.

To get a feeling for the role of dispersion (we cannot carry out a reliable estimate of the dispersion force), the total bonding energy was evaluated by using the DFT dispersion correction introduced by Grimme et al.[24] Two models were tested. In the first model, estimations by PBE0-D were performed for the PBE0-optimized geometry. In the second model, the geometry of $[(I_2)\cdot(I_2)]$ was optimized at the PBE0-D level of theory. In both cases, the geometry was very similar (see the Supporting Information), and the bonding energy was −4 kcal/mol. Thus, the influence of dispersion forces on the total bonding energy appears small. The same was found for the quadrupole−quadrupole interaction, which we calculated to be ∼1 kcal/mol.[25]

Interestingly, possible formation of a bent (L-shape, C_s-symmetry) geometry of Br_4 was proposed by Alvarez, Mota, and Novoa.[26] Donor−acceptor interaction was explicitly considered by these authors as a driving force that brings two Br_2 molecules together in the preferred geometry. The L-shape geometry was also calculated as the most stable isomer for dimers of other dihalogens, $(Cl_2)_2$ and $(F_2)_2$.[27] There is experimental information on the dimers $(Cl_2)_2$,[28] $(Br_2)_2$, and $(F_2)_2$.[29] The first two are found experimentally (by electron diffraction studies) to be polar, the last slightly so.

If we indeed understand the Janus-faced behavior of diiodine, can we use that understanding to enlarge the corpus of known complexes? We turn next to this challenge.

The Way To Make Further Acceptor Diiodine Complexes. Adducts of late transition metal complexes with molecular I_2, in which the latter shows acceptor behavior, exist, as we saw. Yet they are relatively weakly bound; the maximum bonding energy we could reach in our model compounds is −19 kcal/mol.

Becauase the iodine atom is big and soft, the coordinating metal should, probably, be among the late transition metals. We explored two major directions: (i) changes in the organic ligand, and (ii) change of metal center. The bonding energy between the metal center and the diiodine fragment was taken as an indicator of stability. Replacing donor nitrogen atoms by phosphorus did not lead to an increase of the bonding energy, neither did donor substituents on the phenyl ring. We turned then to modification of the metal center. Replacement of the Pt(II) by other metal of the same group 10 (Ni and Pd) did not have the desired effect; the magnitude of the bonding energy was found to be even smaller (−16 kcal/mol for both Ni and Pd derivatives).

Improvement came on going from group 10 to group 9 (Co, Rh, Ir). To keep compounds isoelectronic, the organic ligand was slightly modified to a pyridine as shown in Scheme 3.

Scheme 3

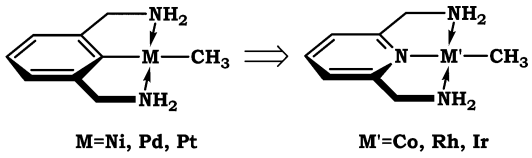

The maximum bonding energy of axial I_2 (−42 kcal/mol) was attained for the Co-derivative; adducts for complexes of other metals of this group gave very similar results, −40 kcal/mol for both Rh and Ir. These are quite large bonding energies; we believe these complexes can be made.

The Way To Make Donor Iodine Complexes, and an Obstacle. As we saw, calculations indicate that iodine donor−acceptor adducts exist, but they are relatively weakly bound. The bonding energy of I_2 with the paddle-wheel complexes ranges between −8 and −13 kcal/mol, depending on the ligand at the end of the complex. The sole experimentally known adduct of I_2 with an organometallic species, $Rh_2(O_2CCF_3)_4$, was obtained only by a "solvent-free" solid/vapor deposition.[3] Even such strong acceptors as $B(CF_3)_3$ and $AlCl_3$ form (in our calculations) adducts with I_2 with relatively low bonding energy (−16 and −9 kcal/mol, respectively).

dx.doi.org/10.1021/ja312584u | J. Am. Chem. Soc. 2013, 135, 3262−3275

What might be the origins of the relatively low stability of these compounds? The main reason, we think, is the high magnitude of the repulsion between the fragments (estimated by ΔE_{Pauli} within the EDA analysis). This contribution is large, and in most cases is as large (or larger) as the electrostatic component of the bonding (Table 6). An iodine atom of I_2 is large and possesses a very diffuse electron density, which we think causes the large repulsion with the electron density of an organometallic, organic, or inorganic acceptor. Such repulsion is negligible for the proton as an acceptor. Indeed the bonding energy there, in HI_2^+, is large, ~ -156 kcal/mol.

How might one modify an organometallic acceptor fragment to make it more suitable for coordination of I_2 as a donor? The I_2 ligand is large and soft (the terminology is of hard/soft Lewis acids/bases). Hence, the metallic center should also be large and soft. This may not solve the problem of a large repulsion, but it will increase the bonding between the fragments. In the transition metal block this means that one should go down and to the right in the Periodic Table.[1] Indeed, a pilot calculation of $[CpIr(CO)\cdot(I_2)]$ shows high stability, with $-D_e = -51$ kcal/mol. Similar results were obtained for the model complex $[CpRe(CO)_2\cdot(I_2)]$, with a bonding energy of −42 kcal/mol. In both cases, the I_2 ligand is coordinated in a bent fashion, evidence of its donor behavior.

However, another problem immediately emerges, the potential of oxidative addition to give a diiodide (Scheme 4).[4,5] Halides are very good ligands, even if there are fewer

Scheme 4

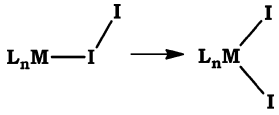

iodides than bromides or chlorides. Indeed, we calculate that oxidative additions in $[CpIr(CO)\cdot(I_2)]$ and $[CpRe(CO)_2\cdot(I_2)]$ to give $[CpIr(CO)\cdot(I)_2]$ and $[CpRe(CO)_2\cdot(I)_2]$ are exothermic by 33 and 20 kcal/mol, respectively. The oxidative addition, as long suspected, is a symmetry-allowed process; that is, there are no level-crossings between reactants and products.[30] Nevertheless, the calculated barrier for the reaction $[CpIr(CO)\cdot(I_2)] \rightarrow [CpIr(CO)\cdot(I)_2]$ of +14 kcal/mol indicates that the adduct of molecular I_2 might be, in principle, stabilized and isolated at low temperature. This result (summarized in Figure 18) is encouraging; we have not yet optimized the potential substituents on Cp and Ir.

Next, we turned to late transition metal complexes in which the metal center is "protected" by ligands as, for example, in original paddle-wheel compound $[Rh_2(O_2CCF_3)_4]$. For these, oxidative addition to the same metal center is not expected; the binuclear paddle-wheel bonding poses, we think, a formidable constraint to achieving a locally seven-coordinated environment at the metal. A set of modified paddle-wheel complexes was tested as potential partners for molecular I_2. The energy of σ^*(M−M) MO (LUMO in most cases) was chosen as an indicator of suitability for bonding with I_2; the lower is the σ^*, the more localized on a metal center, the better. All metals of the same group, Co, Rh, and Ir, were probed in different combinations. Little variation in the energy of the σ^*-LUMO emerged.

We then modified the dimetal core by replacing one of the elements of group 9 by one of group 10 (Ni, Pd, Pt), at the same time capping one open site of paddle-wheel complex by chlorine to stay isoelectronic (Scheme 5). This maneuver

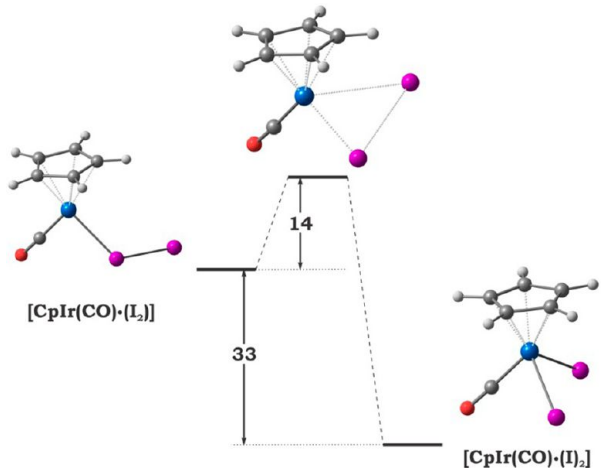

Figure 18. Schematic energy diagram (in kcal/mol) for the oxidative addition process $[CpIr(CO)\cdot(I_2)] \rightarrow [CpIr(CO)\cdot(I)_2]$.

Scheme 5

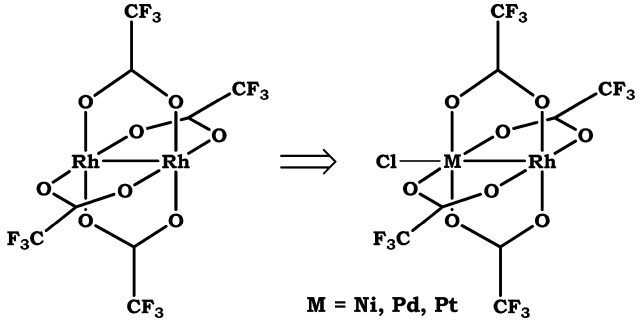

brings the level of LUMO slightly down in energy; the lowest σ^* energy was found for $[RhNi(O_2CCF_3)_4\cdot(Cl)]$ (−5.72 vs −4.59 eV for $[Rh_2(O_2CCF_3)_4]$). The stability of corresponding I_2 adduct was increased just by 2 kcal/mol in comparison with that of the Cotton complex. The result is not spectacular; we will continue our search. Still, this type of paddle-wheel compound as well as the aforementioned $[CpIr(CO)\cdot(I_2)]$ and $[CpRe(CO)_2\cdot(I_2)]$ complexes can be recommended for low temperature synthesis.

CONCLUDING REMARKS

Our detailed theoretical analysis of I_2 adducts with Pt(II) square-planar complexes, where diiodine occupies the fifth axial position, allowed us to unambiguously assign the nature of this interaction. The bonding between I_2 and Pt center is best described as donor−acceptor, in which the dihalogen plays the role of a relatively strong acceptor through the σ^*(I−I) orbital. The platinum fragment takes part in this bonding as a donor, through an orbital mainly d_z^2 in nature. The donor behavior of the metal fragment was found to be an intrinsic feature of d^8-Pt(II) square-planar complexes, when the fifth ligand approaches in an axial mode. The influence of the in-plane ligand is minimal. This statement was supported by variations of the in-plane ligands as well as by variations of the acceptor axial one. The classical $(I_2)\rightarrow$Pt interaction, diiodine acting as donor, is very weak and does not involve the empty p_z-orbital of the metal center as one might anticipate.

dx.doi.org/10.1021/ja312584u | J. Am. Chem. Soc. 2013, 135, 3262−3275

d^8-Pt(II) square-planar complexes tend not to form stable adducts, even with relatively strong donors, approaching at the axial position. Theoretical support for this negative conclusion came from a detailed theoretical investigation of NH_3 approaching the fifth coordination site. The empty p_z-orbital of the Pt(II)-center apparently cannot be activated, even by strong donors.

The acceptor behavior of the I_2 molecule was then confirmed by modeling of its adducts with pure organic donors such as the simplest *N*-heterocyclic carbene and/or substituted amines. A high degree of similarity between the van Koten compounds and these adducts (of amines and NHC) was established. An analogy was sought and found between these complexes in which diiodine acts as an acceptor and BH_3 complexes.

Yet diiodine can also be a donor. Our detailed theoretical analysis of I_2 adducts with the dimetal paddle-wheel complex $[Rh_2(O_2CCF_3)_4]$, based on the single known complex, where diiodine is coordinated at the axial position in a bent fashion, allowed us to unambiguously assign the nature of this interaction. Consistent with its geometry, the bonding between the I_2 and the Rh_2-core is best described as donor−acceptor, where the dihalogen acts as a donor through the lone pair of one of two iodine atoms, a localized p orbital in an NBO picture, and a mixture of π and π^* canonical MOs of the diatomic. The dirhodium core of the metallic fragment plays an acceptor role in this bonding through its σ^*(Rh−Rh) orbital. No contribution from donation in the reverse direction, I_2 acting as an acceptor, was found, completely different from what was observed for three other known I_2 complexes. In the paddle-wheel complexes, the presence of the second axial ligand weakens the target interaction. The stronger donor is the second axial ligand, the weaker is the Rh−I bond.

The donor behavior of the I_2 molecule was then confirmed by modeling its adducts with organic and inorganic acceptors such as $B(CF_3)_3$ and $AlCl_3$. The close resemblance between the complex synthesized by Cotton, Dikarev, and Petrukhina and such adducts, so far hypothetical, was established.

Another part of our study shows the real two-faced nature of the I_2 molecule. Formation of the adduct $[(I_2)\cdot(I_2)]$, bound (albeit weakly so) by donor−acceptor interaction, provided a unique example of a system in which diiodine is a donor and an acceptor, all in one molecule.

Our energy decomposition analysis points to large Pauli repulsion as one explanation for the scarcity of I_2 (or other dihalogen) organometallic complexes. Another reason, long suspected, is the stability of the diiodide products of oxidative addition of coordinated I_2 to the metal center, and the allowed nature of the oxidative addition. We investigated this problem and came up with a strategy for improving M−I_2 bonding, the best candidates so far being $[CpIr(CO)\cdot(I_2)]$ and/or $[Cp(Re(CO)_2\cdot(I_2)]$, and some heterobinuclear paddle-wheel complexes.

It remains pretty remarkable that the number of I_2 complexes can so far be numbered on one hand. Also, that among the four known adducts there are found two entirely different coordination modes, I_2 acting as an acceptor in three cases, as a donor in one. We think this tiny class of organometallics can be induced to grow, and we sketch a design strategy for organometallic fragments that will form more stable I_2 adducts.

■ ASSOCIATED CONTENT

Supporting Information

Computational details; description of EDA analysis; coordinates and energies of the calculated model adducts; NBO charges and Wiberg bond orders for all atoms in the calculated complexes; geometric and EDA parameters for the model Pt(II) complexes; coordinates, energies, and charge analysis for the real complex calculations; optimized coordinates, pictures of geometries, energies, bond orders, and charges for pure organic donors interacting with diiodine; and NBO and EDA analysis of interaction for the same. This material is available free of charge via the Internet at http://pubs.acs.org.

■ AUTHOR INFORMATION

Corresponding Author

rh34@cornell.edu

Notes

The authors declare no competing financial interest.

■ ACKNOWLEDGMENTS

We are grateful to G. van Koten for bringing to our attention a number of important papers and useful comments, and to P. Wolzanski for steering us to the work of A. Heyduk. Our work was supported by the National Science Foundation, Research Grant CHE-0910623. Computational facilities provided by KAUST (King Abdullah University of Science and Technology) Supercomputing Laboratory are gratefully acknowledged.

■ REFERENCES

(1) (a) Crabtree, R. H. *The Organometallic Chemistry of the Transition Metals*; Wiley Inc.: New York, 2009. (b) Hartwig, J. *Organotransition Metal Chemistry*; University Science Books: CA, 2010.

(2) (a) Gossage, R. A.; Ryabov, A. D.; Spek, A. L.; Stufkens, D. J.; van Beek, J. A. M.; van Eldik, R.; van Koten, G. *J. Am. Chem. Soc.* **1999**, *121*, 2488. (b) van Beek, J. A. M.; van Koten, G.; Smeets, W. J. J.; Spek, A. L. *J. Am. Chem. Soc.* **1986**, *108*, 5010. (c) van Beek, J. A. M.; van Koten, G.; Dekker, G. P. C. M.; Wissing, E.; Zoutberg, M. C.; Stam, C. H. *J. Organomet. Chem.* **1990**, *394*, 659−678. (d) van Koten, G. *Pure Appl. Chem.* **1990**, *62*, 1155.

(3) Cotton, F. A.; Dikarev, E. V.; Petrukhina, M. A. *Angew. Chem., Int. Ed.* **2000**, *39*, 2362.

(4) Shaffer, D. W.; Ryken, S. A.; Zarkesh, R. A.; Heyduk, A. F. *Inorg. Chem.* **2012**, *51*, 12122.

(5) Makiura, R.; Nagasawa, I.; Kimura, N.; Ishimaru, S.; Kitagawa, H.; Ikeda, R. *Chem. Commun.* **2001**, 1642.

(6) (a) Harvey, J. N.; Poli, R. *Dalton Trans.* **2003**, 4100. (b) Wang, W.; Narducci, A. A.; House, P. G.; Weitz, E. *J. Am. Chem. Soc.* **1996**, *118*, 8654 and references therein.

(7) Guihaumé, J.; Raynaud, C.; Eisenstein, O.; Perrin, L.; Maron, L.; Tilley, T. D. *Angew. Chem., Int. Ed.* **2009**, *49*, 1816.

(8) Gualco, P.; Lin, T.-P.; Sircoglou, M.; Mercy, M.; Ladeira, S.; Bouhadir, G.; Pérez, L. M.; Amgoune, A.; Maron, L.; Gabbaï, F. P.; Bourissou, D. *Angew. Chem., Int. Ed.* **2009**, *48*, 9892.

(9) (a) Muir, K. W.; Ibers, J. A. *Inorg. Chem.* **1969**, *8*, 1921. (b) Ryan, R. R.; Eller, P. G. *Inorg. Chem.* **1976**, *15*, 494. (c) Mingos, D. M. P. *Trans. Met. Chem.* **1978**, *3*, 1. (d) Ryan, R. R.; Kubas, G. T.; Moody, D. C.; Eller, P. G. *Struct. Bonding (Berlin)* **1981**, *46*, 47.

(10) Geometry optimizations were performed at PBE0/SARC-TZVP level of theory (within RIJCOSX approximation). Scalar relativistic effects have been incorporated by applying the zero-order regular approximation (ZORA). All of these calculations were carried out by using the ORCA program suite (version 2.9.0). Optimized geometries were used to get insight into the electronic structure of our target systems in terms of natural bond orbitals (NBO). Bond orders quoted are those from the Wiberg formulation (so-called Wiberg bond

indexes) incorporated in the NBO analysis. All computations were performed with GENNBO (version 5.0) program, using the converged wave functions generated by ORCA programs. The bonding between metal-based fragment and diiodine was further investigated by the energy decomposition analysis (EDA) developed by Morokuma and by Ziegler and Rauk.[10] For this purpose, single-point calculations were performed by the ADF program package with the same functional. All atoms were described by uncontracted Slater-type orbitals (STOs) with TZ2P quality as basis functions. Throughout our Article, we use as an indicator of stability the bonding energy, $-D_e$, where $-D_e = \Delta E$ for the reaction fragments ↔ molecule. Thus, $-D_e = E(\text{adduct}) - E(\text{metal fragment}) - E(I_2)$, each optimized separately. $-D_e$ is a negative quantity, when the adduct is more stable than the fragments. A full description of computational details can be found in the Supporting Information.

(11) (a) Weinhold, F., Landis, C. A. *Valency and Bonding: A Natural Bond Orbital Donor − Acceptor Perspective*; Cambridge University Press: Cambridge, 2005. (b) Reed, A. E.; Curtiss, L. A.; Weinhold, F. *Chem. Rev.* **1988**, *88*, 899.

(12) (a) Morokuma, K. *J. Chem. Phys.* **1971**, *55*, 1236. (b) Ziegler, T.; Rauk, A. *Inorg. Chem.* **1979**, *18*, 1558. (c) Ziegler, T.; Rauk, A. *Inorg. Chem.* **1979**, *18*, 1755.

(13) Zanni, M. T.; Taylor, T. R.; Greenblatt, B. J.; Soep, B.; Neumark, D. M. *J. Chem. Phys.* **1997**, *107*, 7613.

(14) Svensson, P. H.; Kloo, L. *Chem. Rev.* **2003**, *103*, 1649.

(15) Stromme, K. O. *Acta Chem. Scand.* **1959**, *13*, 268.

(16) Maijsers, J. C.; Niemantsverdriet, J. W.; Wehman-Ooyevaar, I. C. M.; Grove, D. M.; van Koten, G. *Inorg. Chem.* **1992**, *31*, 2655.

(17) (a) Terheijden, J.; van Koten, G.; de Booys, J. L.; Ubbele, H. T. C.; Stam, C. H. *Organometallics* **1983**, *2*, 1882. (b) van Koten, G.; Terheijden, J.; van Beek, J. A. M.; Wehman-Ooyevaar, I. C. M.; Muller, F.; Stam, C. H. *Organometallics* **1990**, *9*, 903. (c) van Beek, J. A. M.; van Koten, G.; Wehman-Ooyevaar, I. C. M.; Smeets, W. J. J.; van der Sluis, P.; Spek, A. L. *J. Chem. Soc., Dalton Trans.* **1991**, 883.

(18) Bickelhaupt, F. M.; Baerends, E. J.; Ravenek, W. *Inorg. Chem.* **1990**, *29*, 350.

(19) (a) Cotton, F. A.; Dikarev, E. V.; Petrukhina, M. A. *J. Am. Chem. Soc.* **2001**, *123*, 11655. (b) Petrukhina, M. A.; Scott, L. T. *Dalton Trans.* **2005**, 2969. (c) Petrukhina, M. A. *Coord. Chem. Rev.* **2007**, *251*, 1690. (d) Filatov, A. S.; Petrukhina, M. A. *Coord. Chem. Rev.* **2010**, *254*, 2234. (e) Petrukhina, M. A.; Andreini, K. W.; Mack, J.; Scott, L. T. *Angew. Chem., Int. Ed.* **2003**, *42*, 3375. (f) Petrukhina, M. A.; Andreini, K. W.; Peng, L.; Scott, L. T. *Angew. Chem., Int. Ed.* **2004**, *43*, 5477. (g) Petrukhina, M. A.; Andreini, K. W.; Tsefrikas, V. M.; Scott, L. T. *Organometallics* **2005**, *24*, 1394. (h) Rogachev, A.Yu.; Petrukhina, M. A. *J. Phys. Chem. A* **2009**, *113*, 5743. (i) Filatov, A. S.; Rogachev, A. Yu.; Jackson, E. A.; Scott, L. T.; Petrukhina, M. A. *Organometallics* **2010**, *29*, 1231. (j) Filatov, A. S.; Rogachev, A.Yu.; Petrukhina, M. A. *Cryst. Growth Des.* **2006**, *6*, 1479.

(20) (a) Albrecht, M.; Lutz, M.; Schreurs, A. M. M.; Lutz, E. T. H.; Spek, A. L.; van Koten, G. *J. Chem. Soc., Dalton Trans.* **2000**, 3797. (b) Albrecht, A.; Lutz, M.; Spek, A. L.; van Koten, G. *Nature* **2000**, *406*, 970.

(21) (a) Wehman-Ooyevaar, I. C. M.; Grove, D. M.; Kooijman, H.; van der Sluis, P.; Spek, A. L.; van Koten, G. *J. Am. Chem. Soc.* **1992**, *114*, 9916. (b) Wehman-Ooyevaar, I. C. M.; Grove, D. M.; de Vaal, P.; Dedieu, A.; van Koten, G. *Inorg. Chem.* **1992**, *31*, 5484.

(22) Hassel, O.; Romming, C. *Q. Rev., Chem. Soc.* **1962**, *16*, 1.

(23) The proton affinity was calculated at the (RIJCOSX)-PBE0/TZVP/ZORA level of theory for all systems. Our results agree reasonably with experimental values for the gas-phase proton affinity (203 kcal/mol for NH_3 and 166 kcal/mol for H_2O) collected in: Lias, S. G.; Liebman, J. F.; Levin, R. D. *J. Phys. Chem. Ref. Data* **1984**, *13*, 695.

(24) Grimme, S.; Antony, J.; Ehrlich, S.; Krieg, H. *J. Chem. Phys.* **2010**, *132*, 154104.

(25) Quadrupole tensors were calculated at the PBE0/TZ2P level of theory with help of the ADF package. All numbers were obtained using the Buckingham convention. Quadrupole tensors were calculated for two I_2 fragments in separate calculations using an optimized geometry for the $[(I_2)\cdot(I_2)]$ pair. The parameter r was taken as the distance between mass centers of the fragments (r = 5.378 Å).

(26) Alvarez, S.; Mota, F.; Novoa, J. *J. Am. Chem. Soc.* **1987**, *109*, 6586.

(27) (a) Prissette, J.; Kochanski, E. *J. Am. Chem. Soc.* **1977**, *99*, 7352. (b) Kochanski, E. *J. Chem. Phys.* **1982**, *77*, 2691. (c) Umeyama, H.; Morokuma, K.; Yamabe, S. *J. Am. Chem. Soc.* **1977**, *99*, 330.

(28) Harris, S. J.; Novick, S. E.; Winn, J. S.; Klemperer, W. *J. Chem. Phys.* **1974**, *61*, 3866.

(29) Chance, K. V.; Bowen, K. H.; Winn, J. S.; Klemperer, W. *J. Chem. Phys.* **1980**, *72*, 791.

(30) (a) Dedieu, A.; Strich, A. *Inorg. Chem.* **1979**, *18*, 2940. (b) Sargent, A. L.; Hall, M. B. *Inorg. Chem.* **1992**, *31*, 317.